IOP Publishing Nanotechnology
Nanotechnology **25** (2014) 485204 (12pp) doi:10.1088/0957-4484/25/48/485204

Effect of intermolecular force on the static/dynamic behaviour of M/NEM devices

Namjung Kim and N R Aluru

Department of Mechanical Science and Engineering, Beckman Institute of Advanced Science and Technology, University of Illinois at Urbana-Champaign, Urbana, IL, USA

E-mail: aluru@illinois.edu

Received 20 June 2014, revised 23 September 2014
Accepted for publication 13 October 2014
Published 14 November 2014

Abstract

Advances made in the fabrication of micro/nano-electromechanical (M/NEM) devices over the last ten years necessitate the understanding of the attractive force that arises from quantum fluctuations (generally referred to as Casimir effects) [Casimir H B G 1948 *Proc. K. Ned. Akad. Wet.* 51 793]. The fundamental mechanisms underlying quantum fluctuations have been actively investigated through various theoretical and experimental approaches. However, the effect of the force on M/NEM devices has not been fully understood yet, especially in the transition region involving gaps ranging from 10 nm to 1 μm, due to the complexity of the force. Here, we numerically calculate the Casimir effects in M/NEM devices by using the Lifshitz formula, the general expression for the Casimir effects [Lifshitz E 1956 *Sov. Phys. JETP* 2 73]. Since the Casimir effects are highly dependent on the permittivity of the materials, the Kramer–Kronig relation [Landau L D, Lifshitz E M and Pitaevskii L P 1984 *Electrodynamics of Continuous Media* (New York: Pergamon Press)] and the optical data for metals and dielectrics are used in order to obtain the permittivity. Several simplified models for the permittivity of the materials, such as the Drude and Lorentz models [Jackson J D 1975 *Classical Electrodynamics* (New York: Wiley)], are also used to extrapolate the optical data. Important characteristic values of M/NEM devices, such as the pull-in voltage, pull-in gap, detachment length, etc, are calculated for devices operating in the transition region. Our results show that accurate predictions for the pull-in behaviour are possible when the Lifshitz formula is used instead of the idealized expressions for Casimir effects. We expand this study into the dynamics of M/NEM devices, so that the time and frequency response of M/NEM devices with Casimir effects can be explored.

Keywords: M/NEMS, pull-in behaviour, casimir effects

1. Introduction

Over the past thirty years, micro-electromechanical systems (MEMS) have gained significant attention due to their potential for high sensitivity in physical, chemical and biological sensing. Recently, even smaller devices have been fabricated leading to the design and development of nano-electromechanical systems (NEMS). These sensors have several advantages over conventional devices in terms of small size, high sensitivity, low cost, low power consumption, and quick response. Therefore, micro/nanoelectromechanical (M/NEM) devices are currently being studied extensively for various applications.

A popular technique to actuate M/NEM devices is to use electrostatic force. Consider an M/NEM device consisting of an elastic movable part, made of a conductive (or semiconductor) material, over a rigid ground electrode, called the substrate. The applied voltage induces an electric field between the electrodes, which results in the build-up of an electrostatic charge on the surface of the electrodes. The electrostatic force, resulting from the induced charge, deflects the movable part of the M/NEM device towards the substrate. If the applied voltage is higher than a critical value, instability occurs and the movable part collapses onto the substrate. The critical values of the voltage and the distance between the movable part and the substrate are called the pull-in voltage and pull-in gap, respectively [5]. This pull-in behaviour is one of the most important phenomena in M/NEM devices.

As the gap distance between the devices gets smaller, the interaction force between the molecules in the movable part

and the substrate becomes important. This intermolecular force can change the deflection, altering the pull-in behaviour. Thus, the pull-in behaviour of devices at small scales should take into account the intermolecular force as well as the elastic and electrostatic forces.

Previous investigations reported the effect of the intermolecular force on the pull-in behaviour in M/NEM devices by employing idealized expressions for the van der Waals and Casimir forces [6–28]. Using a local value approach, Serry *et al* numerically explained the static deflection and collapse of MEM systems by the effect of the Casimir force between the parallel plate and fixed surface [6]. The influence of the Casimir effect with surface roughness, conductivity and temperature changes on the stable/unstable static equilibrium states of MEM systems was analyzed by Ding *et al* [7]. Wang *et al* studied the behaviour of a microfabricated rectangular membrane driven by an electrostatic force with the Casimir force between the conducting surfaces [8]. Buks *et al* experimentally and numerically investigated the Casimir interaction between micromachined Au cantilevers [9]. Spengen *et al* presented a model for stiction in MEM systems due to surface interaction, including the van der Waals force, and other environmental conditions [10].

Dequesnes *et al* studied the static and dynamic behaviour of carbon nanotube-based switches using the Lennard–Jones potential, describing the van der Waals interaction [11, 12]. Guo *et al* investigated the influence of the van der Waals and Casimir forces on the stability of electrostatic torsional NEMS actuators using a simplified one-degree of freedom model [13]. Palasantzas *et al* investigated the influence of self-affine roughness on the pull-in parameters for switches used in M/NEMS in the presence of the Casimir force [14]. Lin and Zhao presented a theoretical analysis of the influence of the Casimir effect on the nonlinear behaviour of nanoscale electrostatic actuators [15]. Ramezani *et al* studied closed form solutions and validation of the pull-in instability of nanomechanical switches [16–18] as well as nanocantilever arrays [19] under intermolecular and electrostatic forces. Batra *et al* analyzed the effects of the Casimir force on the pull-in instability in micromembranes [20], and various shapes of plates [21, 22]. Zand and Ahmadian studied the dynamic pull-in instability of electrostatically actuated beams under intermolecular forces using the idealized expressions of van der Waals and Casimir forces [23]. Wang *et al* proposed a numerical algorithm that can predict the static and dynamic behaviour of circular M/NEM devices under the influence of electrostatic and Casimir forces [24]. Recently, Koochi *et al* studied the analytical modeling of the pull-in instability of the CNT probe/actuator with the van der Waals force [25]. More details on the pull-in instability of M/NEM devices including Casimir effects are discussed in [26–28]. Reference [26] reviews the theoretical details of Casimir effects as well as experimental observations and applications. Reference [28] describes the pull-in instability under electrostatic force, and [27] discusses stiction and other factors that should be considered in M/NEM devices.

In 1940, H G Casimir derived a general expression for intermolecular force, which unifies the idealized expressions for intermolecular forces, i.e. the van der Waals and Casimir forces, by using quantum fluctuation [1]. In the original Casimir derivation, the presence of two perfectly conducting plates quantizes the field mode inside the plates, so the attractive force is derived from the total energy difference between the field inside and outside of the plates. In this approach, the force F_c between two perfectly conducting plates is proportional to the surface area A of the plates, the reduced Planck constant $\hbar$ and the speed of light c:

$$F_c = A\frac{\hbar c\pi^2}{240l^4}. \quad (1)$$

The interesting aspect of this expression is that the force varies inversely proportional to the fourth power of gap l, and independent of the material properties. Casimir's original result assumed that the plates are perfect conductors, which do not allow electric fields to penetrate them. However, any material becomes transparent at sufficiently high frequencies due to the finite value of its conductivity [3]. The finite value of conductivity introduces the necessity of a correction factor for the Casimir force, which is not needed when assuming perfectly conducting metals.

Lifshitz provided a general description of the van der Waals and Casimir interaction between two bodies in terms of the permittivity of materials [2]. The allowed field mode frequencies can be obtained by considering the material properties and boundary conditions for the electromagnetic field. After deriving the interaction energy for each mode, the summation over all the allowed modes is done to get the energy difference between the inside and outside of the two plates. The interaction force from the Lifshitz formula is the derivative of the energy difference with respect to the gap distance. Zhou and Spruch derived a generalized form of the quantized field modes between multilayered walls in terms of permittivities of media [29]. The more general derivation of the Casimir effects in the presence of a background field was proposed to remove the controversy regarding divergence at the boundary [30].

The Lifshitz formula is used to calculate the Casimir effects because it depends not only on the gap distance, but also on the material properties. At gaps smaller than the plasma wavelength (for a metal) or the absorption wavelength (for a dielectric), the force due to quantum fluctuations is properly described using the idealized van der Waals model, which is inversely proportional to the third power of the gap. As the gap increases and the retardation effect becomes significant ($l > 1\ \mu$m), the force is described by the idealized Casimir model, which is inversely proportional to the fourth power of the gap. However, none of these idealized force expressions, such as the van der Waals ($\sim 1/l^3$) and Casimir forces ($\sim 1/l^4$), can describe the force properly in the transition region.

In this paper, we study the static/dynamic behaviour of M/NEM devices accounting for the intermolecular force. Since the presence of the intermolecular force changes the static/dynamic response of the device significantly, we use the Lifshitz formula to account for the complex dependence on

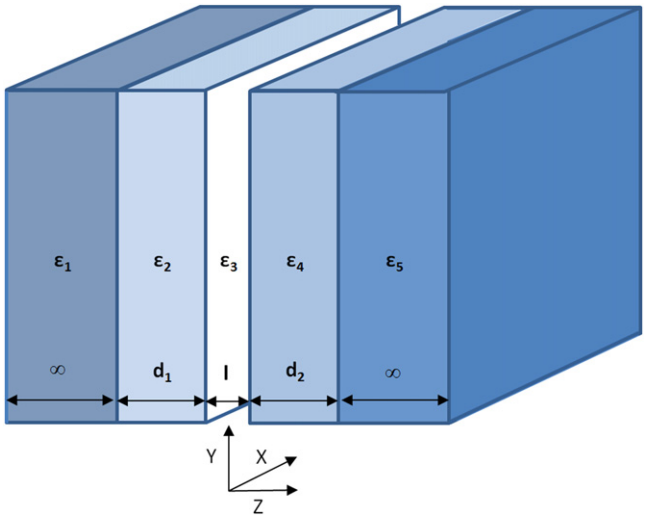

Figure 1. Configuration of a five-layer structure.

the gap distance and the material properties. The rest of the paper is outlined as follows: section 2 presents the Lifshitz formula for the Casimir effects in a five-layer structure. Section 3 describes the permittivities of the metals and dielectrics that are required in order to calculate the Casimir effects in M/NEM devices. Section 4 presents results of the static response of M/NEM devices using a mass-spring-damper (MSD) model, including the pull-in voltage, the pull-in gap, and the detachment length. The dynamic response of M/NEM devices is also presented, including a discussion on the consequences of the Casimir effect on the nonlinear dynamic properties. Conclusions are presented in section 5.

2. Casimir effect in multi-layered planar systems

Figure 1 shows the configuration of a five-layer structure, so that we can consider the interaction force between two semi-infinite spaces (layers 1 and 5) covered with different media (layers 2 and 4). The gap between layers 2 and 4 is l. We set the z-direction as the wave propagation direction, and the xy-plane is perpendicular to the z-axis. In this study, we ignore the temperature effect on the Casimir force to simplify our calculation. It has been reported that the temperature effect is smaller than 5% when the gap distance is less than 1 μm [31].

Following the original Lifshitz derivation, the infinite vacuum energy of the electromagnetic field depends on the gap distance and the thickness of the dielectric layers [32], i.e.

$$E\left(l, d_1, d_2\right) = \frac{1}{2}\hbar\sum_{\underline{k},n}\left(\omega^{(1)}_{\underline{k},n} + \omega^{(2)}_{\underline{k},n}\right), \tag{2}$$

where n is the index of the field mode, and $\underline{k} = (k_1, k_2)$ is the two-dimensional propagation vector in the xy-plane. Indices (1) and (2) stand for two different polarizations of the electric field, which are parallel and perpendicular to the plane formed by $\underline{k}$ and the z-axis, respectively. The vacuum energy density of the electromagnetic field per unit area of the bounding plates is the summation of $E(l, d_1, d_2)$ over all the propagation vector directions:

$$\begin{aligned} E_{total}\left(l, d_1, d_2\right) &= \frac{E\left(l, d_1, d_2\right)}{Area} \\ &= \frac{\hbar}{2}\int\frac{dk_1dk_2}{(2\pi)^2}\sum_{\underline{k},n}\left(\omega^{(1)}_{\underline{k},n} + \omega^{(2)}_{\underline{k},n}\right) \\ &= \frac{\hbar}{4\pi}\int_0^\infty kdk\sum_{\underline{k},n}\left(\omega^{(1)}_{\underline{k},n} + \omega^{(2)}_{\underline{k},n}\right). \end{aligned} \tag{3}$$

The last integration stands for the dimensionless radial coordinate in the $\underline{k}$-plane, and k is the magnitude of $\underline{k}$.

In order to obtain the vacuum energy density we need to calculate the quantized field mode frequencies $\omega^{(1,2)}_{\underline{k},n}$. The Maxwell equations [4] in free space, written for the electric ($\underline{E}$) and magnetic ($\underline{B}$) fields are

$$\begin{aligned} &\nabla\cdot\underline{E} = 0,\ \nabla\times\underline{E} + \frac{1}{c}\frac{\partial\underline{B}}{\partial t} = 0,\ \nabla\cdot\underline{B} = 0,\ \nabla \\ &\times\underline{B} - \frac{1}{c}\frac{\partial\underline{E}}{\partial t} = 0. \end{aligned} \tag{4}$$

The orthonormalized set of the solutions of the Maxwell equations is considered to obtain the surface modes propagating parallel to the surface of the walls. The z-directional vector functions $f_i^{(1,2)}$ and $g_i^{(1,2)}$, which are solutions of the Maxwell equation should satisfy the wave equation [3],

$$\begin{aligned} &\frac{d^2f_i^{(1,2)}}{dz^2} - R_i^2 f_i^{(1,2)} = 0, \\ &\frac{d^2g_i^{(1,2)}}{dz^2} - R_i^2 g_i^{(1,2)} = 0, \end{aligned} \tag{5}$$

where

$$R_i^2 = k^2 - \varepsilon_i(\omega)\frac{\omega^2}{c^2}, \tag{6}$$

i is the index denoting different medium and $\varepsilon_i(\omega)$ is the permittivity of the medium. In our case, i changes from 1 to 5. The boundary conditions at the interface between two dielectrics, i.e. the continuity conditions of the normal and tangential components of the electric and magnetic fields, give the quantized frequencies of the parallel and perpendicular polarizations of the surface modes [31]. Then the quantized frequencies of the surface modes for the five-layer structure can be obtained using the expressions:

$$\begin{aligned} \Omega\left(\omega^{(1,2)}_{\underline{k},n}\right) &= 1 - \frac{q_{23}^{(1,2)} - \bar{q}_{21}^{(1,2)}}{1 - q_{23}^{(1,2)}\bar{q}_{21}^{(1,2)}}\frac{q_{43}^{(1,2)} - \bar{q}_{45}^{(1,2)}}{1 - q_{43}^{(1,2)}\bar{q}_{45}^{(1,2)}}\mathrm{e}^{-2lR_3} \\ &= 0, \end{aligned} \tag{7}$$

where

$$\bar{q}_{21}^{(1,2)} = q_{21}^{(1,2)}\mathrm{e}^{-2d_1R_2},\ \bar{q}_{45}^{(1,2)} = q_{45}^{(1,2)}\mathrm{e}^{-2d_2R_4}, \tag{8}$$

$$q_{21}^{(1,2)} = \frac{\left(r_{21}^-\right)^{(1,2)}}{\left(r_{21}^+\right)^{(1,2)}},\ q_{23}^{(1,2)} = \frac{\left(r_{23}^-\right)^{(1,2)}}{\left(r_{23}^+\right)^{(1,2)}},$$

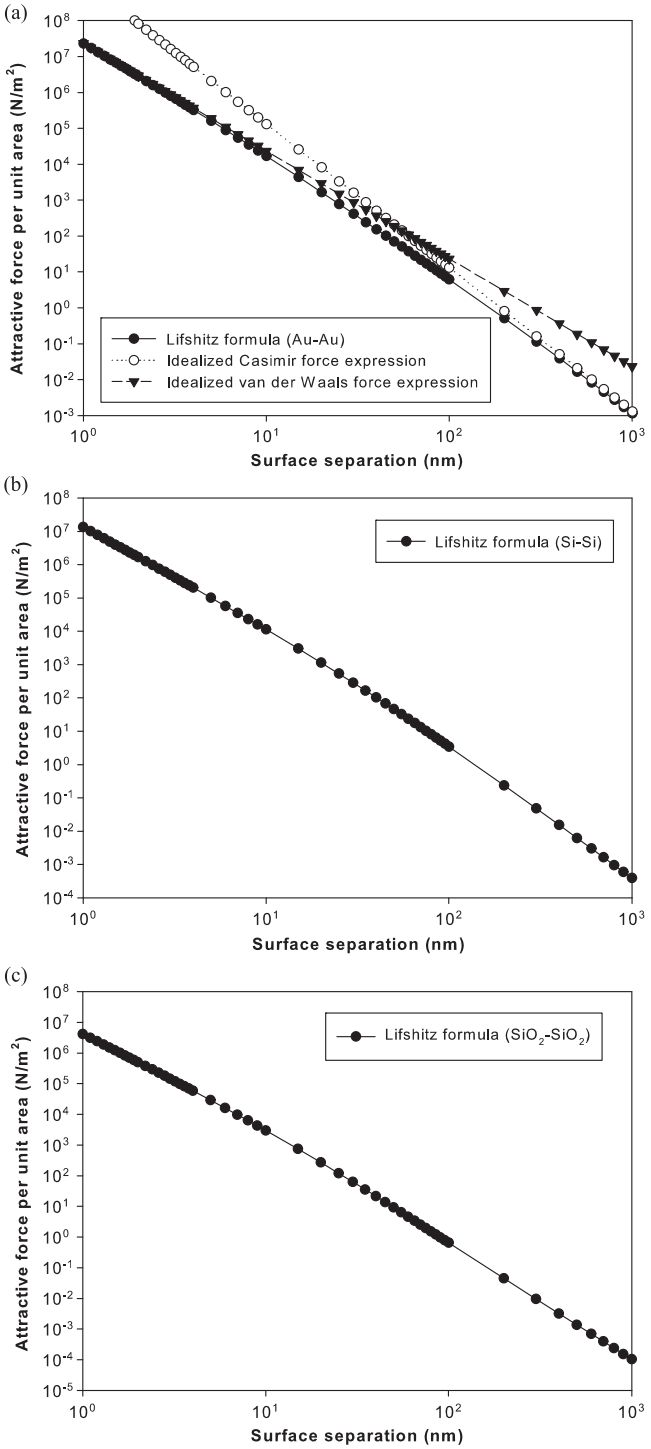

Figure 2. The absolute value of the attractive force between two semi-infinite plates ((a) Au, (b) Si, and (c) SiO_2) as a function of surface separation: the attractive force from the Lifshitz formula (solid circle), the idealized Casimir force expression (open circle), and the idealized van der Waals force expression (solid triangle).

$$q_{43}^{(1,2)} = \frac{\left(r_{43}^{-}\right)^{(1,2)}}{\left(r_{43}^{+}\right)^{(1,2)}},\ q_{45}^{(1,2)} = \frac{\left(r_{45}^{-}\right)^{(1,2)}}{\left(r_{45}^{+}\right)^{(1,2)}}, \tag{9}$$

$$\left(r_{21}^{\pm}\right)^{(1)} = \varepsilon_1 R_2 \pm \varepsilon_2 R_1,\ \left(r_{23}^{\pm}\right)^{(1)} = \varepsilon_3 R_2 \pm \varepsilon_2 R_3,$$
$$\left(r_{43}^{\pm}\right)^{(1)} = \varepsilon_3 R_4 \pm \varepsilon_4 R_3,\ \left(r_{45}^{\pm}\right)^{(1)} = \varepsilon_5 R_4 \pm \varepsilon_4 R_5, \tag{10}$$

$$\left(r_{21}^{\pm}\right)^{(2)} = R_2 \pm R_1,\ \left(r_{23}^{\pm}\right)^{(2)} = R_2 \pm R_3,$$
$$\left(r_{43}^{\pm}\right)^{(2)} = R_4 \pm R_3,\ \left(r_{45}^{\pm}\right)^{(2)} = R_4 \pm R_5. \tag{11}$$

The argument theorem changes the summation of the quantized modes to an integration over the real and imaginary frequency domain [33, 34].

$$\sum_n \left(\omega_{\underline{k},n}^{(1)} + \omega_{\underline{k},n}^{(2)}\right) = \frac{1}{2\pi}\int_{\infty}^{-\infty} \xi d\,\ln \Omega^{(1,2)}(i\xi) + \frac{2}{\pi}\int_{C+} d\xi. \tag{12}$$

The first and second terms on the right-hand side denote the integrations over the imaginary and real frequency domains, respectively. However, the divergence of the summation in equation (12) should be removed. The divergence comes from the first and second terms because of the integration domain. This procedure is called the renormalization. The renormalization procedure removes the divergence in the Casimir energy density by substituting the Casimir energy density when $l \to \infty$ [31].

$$\left(\sum_n \omega_{\underline{k},n}^{(1,2)}\right)_{ren} = \sum_n \omega_{\underline{k},n}^{(1,2)} - \lim_{l\to\infty} \omega_{\underline{k},n}^{(1,2)} = \frac{1}{2\pi}\int_{-\infty}^{\infty} d\xi \ln \frac{\Omega^{(1,2)}(i\xi)}{\Omega_{\infty}^{(1,2)}(i\xi)}. \tag{13}$$

Therefore, the attractive force from the Casimir energy density across the gap in the five-layer structure can be calculated from equation (3) as follows:

$$F(l, d_1, d_2) = -\frac{dE_{total}(l, d_1, d_2)}{dl} = -\frac{\hbar}{2\pi^2}\int_0^{\infty} kdk \int_0^{\infty} d\xi R_3 \times \sum_{\alpha=1,2} \left(\left(\left(q_{23}^{\alpha} - \bar{q}_{21}^{\alpha}\right)\left(q_{43}^{\alpha} - \bar{q}_{45}^{\alpha}\right)e^{-2lR_3}\right) \Big/ \left(\left(1 - q_{23}^{\alpha}\bar{q}_{21}^{\alpha}\right)\left(1 - q_{43}^{\alpha}\bar{q}_{45}^{\alpha}\right) - \left(q_{23}^{\alpha} - \bar{q}_{21}^{\alpha}\right) \times \left(q_{43}^{\alpha} - \bar{q}_{45}^{\alpha}\right)e^{-2lR_3}\right)\right). \tag{14}$$

We can further simplify equation (14) by introducing new variables that are related to the permittivities of the medium [29].

It is well known that this result is the generalized expression for the van der Waals and Casimir forces, depending on the gap distance. First, we can convert equation (14), which is the attractive force for the five-layer structure, into the result for the three-layer structure in the

limit $d_1, d_2 \to \infty$:

$$F(l, d_1, d_2) = -\frac{dE_{total}(l, d_1, d_2)}{dl} = -\frac{\hbar}{2\pi^2}\int_0^\infty kdk \int_0^\infty d\xi R_3 \times \sum_{\alpha=1,2}\left(\frac{\left(q_{23}^\alpha q_{43}^\alpha\right)e^{-2lR_3}}{1-\left(q_{23}^\alpha q_{43}^\alpha\right)e^{-2lR_3}}\right). \quad (15)$$

This equation can be further reduced to the van der Waals force expression by assuming the dielectrics of layer 2 and 4 to be identical ($\varepsilon_2 = \varepsilon_4 = \varepsilon$), and separated by a vacuum ($\varepsilon_3 = 1$). If the absorption wavelength of the dielectric media is smaller than the gap distance ($l \ll c/\omega_0$), equation (15) can be simplified to

$$F_{vdW} = -\frac{H}{6\pi l^3}, \quad (16)$$

where the Hamaker constant H is [32]

$$H = \frac{3\hbar}{8\pi}\int_0^\infty x^2 dx \int_0^\infty d\xi \left(\frac{x^2}{\left(\frac{\varepsilon+1}{\varepsilon-1}\right)^2 e^x - 1}\right). \quad (17)$$

If the absorption wavelength is larger than the gap distance and both plates are perfectly conducting and separated by a vacuum ($\varepsilon_2 = \varepsilon_4 = \infty$, $\varepsilon_3 = 1$), the force is reduced to equation (1), which is the idealized expression of the Casimir force.

Figure 2 shows the absolute value of the Casimir force per unit area as a function of the distance between plates. In addition to the results from the Lifshitz formula, the results from the idealized force expression, such as for the van der Waals ($\sim 1/l^3$) and Casimir forces ($\sim 1/l^4$), are also plotted in figure 2(a). The Casimir force between two semi-infinite gold plates changes slope smoothly from $1/l^3$ to $1/l^4$. At small separations (2–5 nm), the calculations from the van der Waals force approximately match the result from the Lifshitz formula. On the other hand, at large gaps, the results from the idealized Casimir expression deviate by a constant from those of the Lifshitz formula, due to the absence of the finite conductivity effect. Even though the absolute value of the attractive force is different depending on the permittivity, the qualitative behaviour of the curve is the same for metals and dielectrics.

3. Electric permittivities of metals and dielectrics

To evaluate the force with the Lifshitz formula, one needs to know the permittivity of the material. There are three choices in order to calculate the dielectric properties: (1) plasma model, (2) Drude model, and (3) tabulated optical data. The plasma model, which is the one Lifshitz used to calculate the Casimir effects of the real material, is often used [2]. However, the dissipative mechanism of the material is not taken into account in this model and it is proper only at separation distances larger than the plasma wavelength [35]. On the other hand, the Drude model describes the dielectric properties by a set of oscillators, but it has an issue regarding the contradiction with the third law of thermodynamics [36, 37]. Some researchers suggest a mixed model, called the generalized plasma-like dielectric permittivity, to describe the dissipation mechanism at shorter separations [38, 39].

Recent study shows that the dielectric properties of Au films are highly sensitive to the manufacturing process, including annealing and deposition method, so it is very important to use the dielectric permittivity from the samples, which are used for the Casimir force measurement [40, 41].

Since the debate is still going on and there is no final conclusion about the way to decide the dielectric permittivity, in this paper, we use the tabulated optical data with the Drude model for extrapolation, which is a generally well-accepted way to calculate the dielectric permittivity of metals. More details regarding the advantages and disadvantages of the Drude and plasma model can be found in reference [42].

For a homogeneous material, the permittivity is a function of the field mode frequency. If we denote the permittivity as a complex function ($\varepsilon(\omega) = \varepsilon'(\omega) + i\varepsilon''(\omega)$), the dependence of the permittivity on the imaginary part can be written by using the dispersion relation (the so-called Kramer–Kronig relation) [3]:

$$\varepsilon(i\xi) = 1 + \frac{2}{\pi}\int_0^\infty \frac{\omega\varepsilon''(\omega)}{\omega^2+\xi^2}d\omega. \quad (18)$$

The tabulated data for the complex refractive indices of metals and dielectrics in Palik's work [43] are used with the dispersion relation to calculate permittivity on the imaginary frequency axis. The dispersion relation can be used when the experimental data are available for the imaginary part of the permittivity $\varepsilon''(\omega)$ over the full range of integration. In order to calculate the integral in equation (18), the continuous function of permittivity over the frequency is needed. However, the experimental data is discrete and limited in a small frequency range; thus, we perform extrapolation and interpolation of the data for integration purpose. As mentioned above, the Drude model (19) is used for metals, and the Drude-Lorentz model (20) [44] is used to extrapolate the permittivities for silicon.

$$\varepsilon(i\xi) = 1 + \frac{\omega_p^2}{\xi(\xi+\gamma)}, \quad (19)$$

$$\varepsilon(i\xi) = \varepsilon_\infty + \frac{(\varepsilon_0-\varepsilon_\infty)\omega_c^2}{\xi^2+\omega_c^2}, \quad (20)$$

where ω_p is the plasma frequency of the medium, γ is the relaxation parameter, ε_0 is the static permittivity of the substrate, and ε_∞ is the permittivity when the field mode frequency is infinity, and ω_c is the cutoff frequency. For SiO_2, the Ninham–Parsegian model (equation (21)) is used [45]:

Table 1. Parameters of oscillator models.

	ω_p(eV)	γ(eV)				
Au	9.0	0.035				
	ε_0(eV)	ε_∞(eV)	ω_c(eV)			
Si	11.65	1.035	4.325			
	C_1	C_2	C_3	ω_1 (eV)	ω_2 (eV)	ω_3 (eV)
SiO_2	0.829	0.095	1.098	0.3586	0.6238	84.1343

$$\varepsilon(i\xi) = 1 + \sum_i \frac{C_i}{1 + \left(\xi/\omega_i\right)^2}, \tag{21}$$

where coefficient C_i is the oscillator strength and ω_i is the resonance frequency of the ith oscillator. The summation includes two or three oscillator functions, representing different parts of the refractive index plot (ultraviolet, infrared, and microwave). The sum of the oscillator strength should satisfy the relation $\sum_i C_i = \varepsilon_0 - 1$, with ε_0 being the static permittivity of the substrate. The plasma frequency and relaxation parameters as well as other parameters for the metals and dielectrics are described in table 1. Data is linearly interpolated in a logarithmic scale to eliminate fluctuations [35].

The computed permittivities of various metals and dielectrics are plotted in figure 3. The frequency of the electromagnetic field is in electron volts (eV) and is related to its photon energy (1 eV≅2.4×10^{14} Hz). The frequency of the electromagnetic field is related to electron volts through the photoelectric effect ($E = \hbar\nu$). It is well-known that the major contribution to the Casimir force comes from the frequencies around the characteristic frequency ξ, which is determined by the gap distance l and the speed of light $c(\xi = c/2l)$ [32]. The plots of the dielectric permittivity shown in figure 3 correspond to the gap distance 10 nm$< l <$ 1 μm for M/NEM devices in vacuum.

For the permittivity, the major difference between metals and dielectrics is the low-frequency behaviour. While metals, such as gold and aluminum, become perfect mirrors with permittivities approaching infinity, the permittivities of Si and SiO_2 converge to values of 11.65 and 4.09, respectively. The static permittivities of dielectrics can be calculated from the dispersion relation if the experimental data is known, or calculated by using the oscillator models. Before the frequency reaches the cutoff frequency, the permittivities of Si and SiO_2 are nearly constant. Above the cutoff frequency, dielectric permittivities of all materials decrease continuously with increasing frequency until they reach the asymptotic value of about 1, which means that materials become transparent to electromagnetic waves at large frequencies.

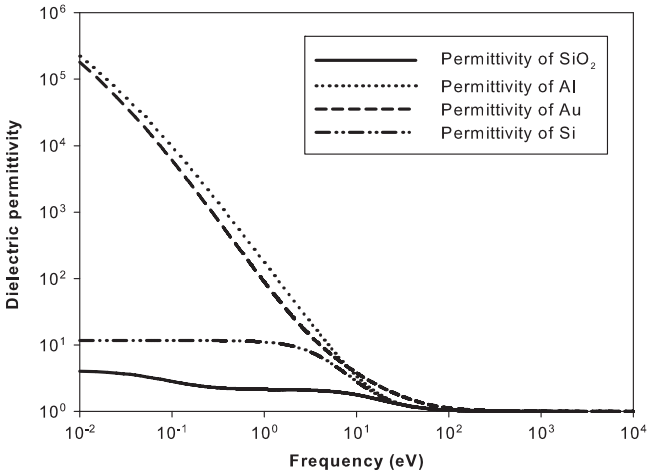

Figure 3. Permittivity as a function of frequency for Au (dashed line), Al (dotted line), Si (dash-dot line), and SiO_2 (solid line) calculated from Kramer–Kronig relations with the optical data.

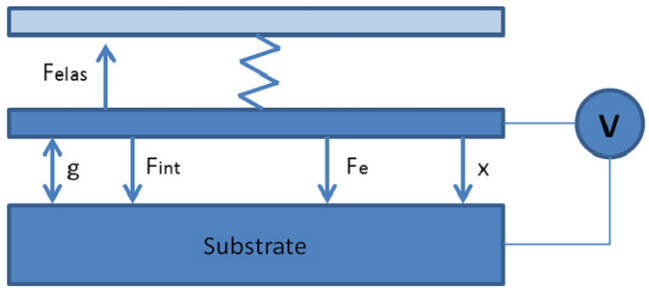

Figure 4. The mass-spring-damper (MSD) model to estimate pull-in parameters of M/NEM switches.

4. Static and dynamic analysis of M/NEM devices

To understand the static and dynamic response of M/NEM devices, the geometry of a cantilever-type switch is modeled as an MSD system (see figure 4). A simpler MSD system is used since the purpose of this work is to understand the effects of the intermolecular force on the M/NEM devices. References [46, 47] contain details on determining the parameters for the distributed system. A more accurate description of M/NEM devices can be obtained by using higher order models such as the finite element model. In the MSD model, the M/NEM devices are approximated as a rigid plate suspended over the substrate, and the elastostatic force is balanced with the electrostatic and intermolecular force at the equilibrium position. The governing equation of the MSD

model is given as:

$$\ddot{x} + 2\varsigma\omega_0\dot{x} + \omega_0^2 x = \frac{1}{m}\left(F_e + F_{\text{int}}\right), \tag{22}$$

where x is the displacement (see figure 4), ω_0 is the resonant frequency of the switch, ς is the damping coefficient, and m is the mass.

If the electrostatic force F_e consists of the dc and ac voltage (V_{dc} and V_{ac}, respectively), the force can be expressed as:

$$F_e = \frac{\varepsilon A}{2(l-x)^2}\left(V_{dc} + V_{ac}\cos(\omega t)\right)^2, \tag{23}$$

where ε is the permittivity of the medium, and ω is the applied frequency. The initial gap distance l is defined as the gap distance without the effect of the intermolecular force and the electrostatic force.

The general way to express the intermolecular force F_{int} is by using the Lifshitz formula as discussed in the previous section. In addition to the Lifshitz formula, the intermolecular force F_{int} can be reduced to the idealized Casimir force $F_{casimir}$ or the van der Waals force F_{vdW} depending on the initial gap distance, i.e.

$$\begin{aligned} F_{\text{int}} = F_{casimir} &= \frac{\pi^2\hbar c A}{240(l-x)^4}, \\ F_{\text{int}} = F_{vdW} &= \frac{HA}{6\pi(l-x)^3}. \end{aligned} \tag{24}$$

The possible interaction between the intermolecular force and the applied electric field is ignored since the operating frequencies of the applied electric field ($\sim 10^6$ Hz) are much smaller than the frequencies at which the intermolecular force is considered ($\sim 10^{14}$ Hz). In addition, the applied voltage is not high enough to cause dielectric break-down or nonlinear effects.

The experimental [48] and analytical [49] studies showed that the tunneling current flow can be established when the tip of the movable part is close to the substrate (~0.7 nm). This tunneling current flow reduces the applied voltage, resulting in the pull-out phenomenon. In our study, we do not consider the unstable state near the substrate, including the pull-out, or contact phenomenon of the device. In addition, the gap distances considered in this study range from 10 nm to 1 μm, therefore the pull-in gap will not reach the limit where the tunneling currents become important.

4.1. Static pull-in behaviour of M/NEM devices

Since the pull-in instability is one of the most important phenomenon in M/NEM devices, the pull-in behaviour needs to be carefully studied. For the static response of M/NEM devices, the ac voltage, mass, and damping terms in equation (22) and equation (23) are ignored. A cantilever type Au nanoswitch is considered to study the static pull-in behaviour of M/NEM devices. The geometrical properties of the nanoswitch are given in table 2. E is Young's modulus.

Table 2. Geometrical properties of the cantilever Au nanoswitch.

Length (nm)	Thickness (nm)	Gap (nm)	E (GPa)
500	10	30	79

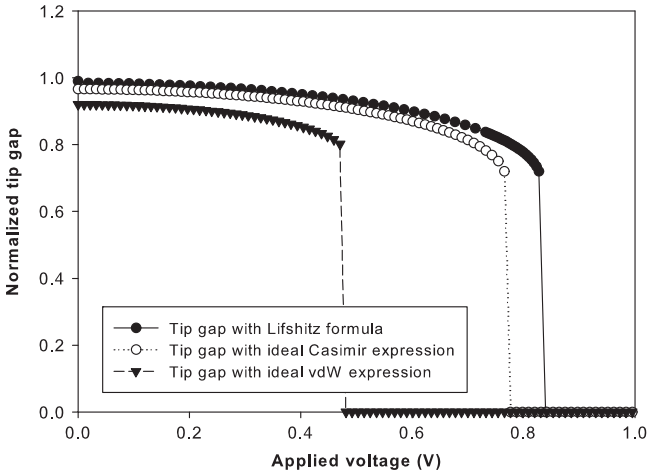

Figure 5. The normalized tip gap distance as a function of the applied voltage with Lifshitz formula (solid circle), the idealized Casimir force expression (open circle), and the idealized van der Waals force expression (solid triangle) using the MSD model.

The Hamaker constant for the van der Waals force [17] is 4.4×10^{-19}.

First, we consider the normalized tip gap distance with different force expressions. The normalized tip gap is defined as the ratio of the deformed gap distance over the initial gap distance. Figure 5 shows the normalized tip gap distance when the intermolecular force is modeled by using the Lifshitz formula, the idealized Casimir force expression, and the idealized van der Waals force expression. Due to the intermolecular force, there are small deviations in the initial gap distance when the applied voltage is 0. Since the initial gap distance (30 nm) is in the transition region, none of idealized expressions for the intermolecular force can predict the pull-in voltage precisely. Pull-in voltages are underestimated by about 10% and 50% when the idealized expressions for the van der Waals and Casimir forces are used, respectively.

Second, the pull-in gap and pull-in voltage as a function of the beam length are studied with different force expressions. Figure 6 shows the variation of the normalized pull-in gap for the cantilever type Au nanoswitch with respect to the beam length. The normalized pull-in gap is defined as the ratio of the pull-in gap distance, which is the gap distance when the pull-in happens, over the initial gap distance. If the normalized pull-in gap is 1, the switch collapses to the substrate. The initial gap distance is 50 nm and the thickness of the switch is 100 nm. The other parameters are the same as those in table 2. If the length of the switch is small, the normalized pull-in gap is the same in all cases and matches with the result obtained when only an electrostatic force is present. However, as the length increases, the normalized pull-in gap increases and the deviation between the result

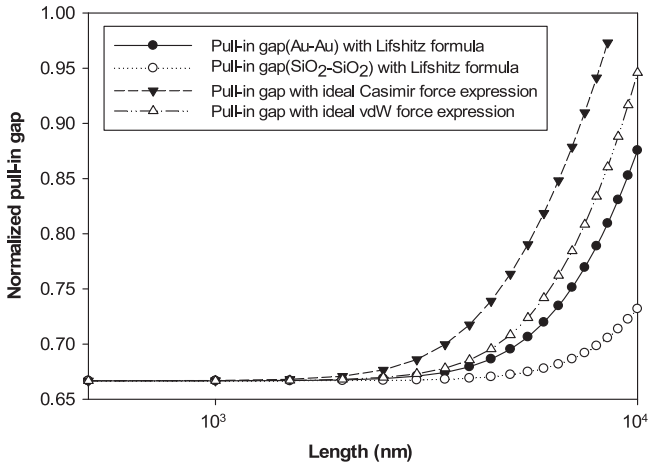

Figure 6. The normalized pull-in gap distance as a function of the beam length with the Lifshitz formula between two semi-infinite gold plates (solid circle), the Lifshitz formula between two semi-infinite SiO_2 plates (open circle), the idealized Casimir force expression (solid triangle), and the idealized van der Waals force expression between two semi-infinite gold plates (open triangle).

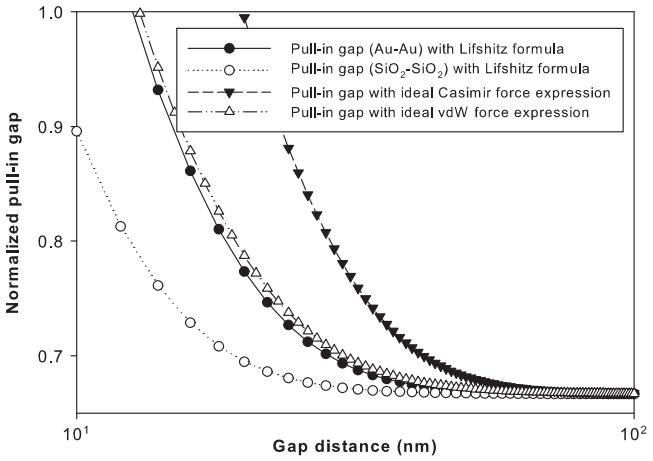

Figure 8. The normalized pull-in gap as a function of the initial gap distance with the Lifshitz formula between two semi-infinite gold plates (solid circle), the Lifshitz formula between two semi-infinite SiO_2 plates (open circle), the idealized Casimir force expression (solid triangle), and the idealized van der Waals force expression between two semi-infinite gold plates (open triangle).

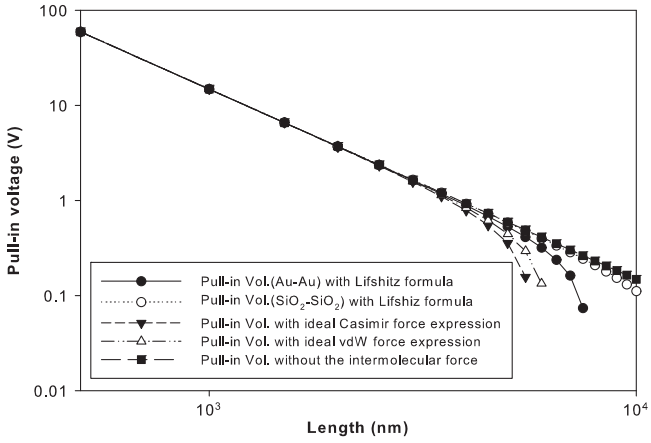

Figure 7. The pull-in voltage as a function of the beam length with the Lifshitz formula between two semi-infinite gold plates (solid circle), the Lifshitz formula between two semi-infinite SiO_2 plates (open circle), the idealized Casimir force expression (solid triangle), and the idealized van der Waals force expression between two semi-infinite gold plates (open triangle). The long dotted line with squares shows the pull-in voltage without the intermolecular force.

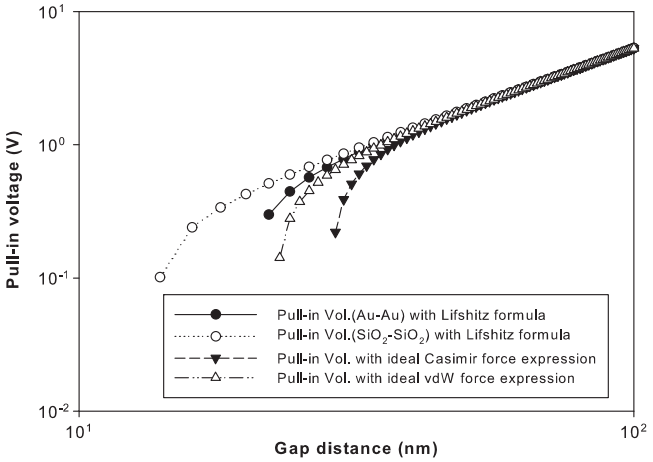

Figure 9. The pull-in voltage as a function of the initial gap distance with the Lifshitz formula between two semi-infinite gold plates (solid circle), the Lifshitz formula between two semi-infinite SiO_2 plates (open circle), the idealized Casimir force expression (solid triangle), and the idealized van der Waals force expression between two semi-infinite gold plates (open triangle).

from the Lifshitz formula and the idealized expressions becomes significant. The idealized Casimir force expression fails to predict the pull-in gap when the length is 10 μm.

Figure 7 shows the pull-in voltage as a function of the beam length with different force expressions. The pull-in voltage is calculated by solving equation (22) and the pull-in gap is shown in figure 6. As shown in figure 7, when the length is small, the effect from the intermolecular force is negligible, and the pull-in voltages with the intermolecular force are identical with the electrostatic force only case. On the other hand, the pull-in voltage is significantly different when the length is greater than 5 μm. Since the idealized Casimir and van der Waals force expressions over-predict the intermolecular force, pull-in occurs at much lower voltages, compared with the results from the Lifshitz formula.

Third, we consider the pull-in gap (figure 8) and pull-in voltage (figure 9) as a function of the initial gap distance with different force expressions. When the initial gap is large enough to make the intermolecular force insignificant, all the normalized pull-in gaps and pull-in voltages are identical with that of the electrostatic force only case on the switch. When the initial gap decreases, the effect of the intermolecular force on both the pull-in gap and the pull-in voltage becomes much clearer. Figure 8 shows that the normalized pull-in gap increases as the intial gap decreases. The idealized Casimir and van der Waals force expressions

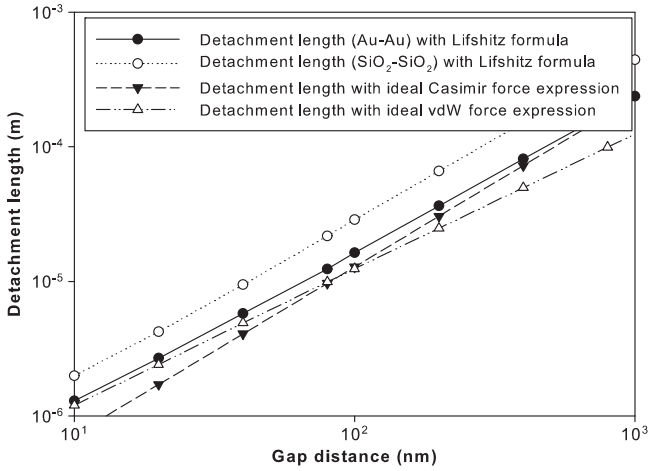

Figure 10. The detachment length of Au and SiO_2 movable parts on the substrate in the transition region (from 10 nm to 1 μm).

fail to describe the pull-in behaviour of the switch for lengths between 10 and 100 nm.

4.2. Detachment length of M/NEM devices

Detachment length of a given tip gap is defined as the maximum length of an M/NEM device that does not stick to the substrate without an applied voltage [50]. Therefore, detachment length is one of the important design parameters of M/NEM devices. Previous work computed the detachment length of M/NEM devices using the idealized Casimir [50] or van der Waals force expressions [17]. However, if the initial gap distance is within the transition region, the intermolecular force is also affected by the material properties of devices.

The detachment length is calculated from equation (22) with the Lifshitz formula. The thickness of the switch is 100 nm and all other parameters are the same as those in table 2. Figure 10 shows the detachment lengths calculated from the Lifshitz formula (Au-Au and SiO_2-SiO_2) and the one calculated with the idealized Casimir force and van der Waals expressions. The results from the Lifshitz formula (Au-Au) indicate that the slope changes smoothly from 3 to 4, which are the slopes from the idealized expressions of the van der Waals and Casimir forces, respectively. When the gap is close to 1 μm, the detachment length matches with that of the idealized Casimir force expression. However, as the initial gap gets smaller, the results from the Lifshitz formula deviate from those of the idealized Casimir force expression, and it converges to the detachment length that is calculated from the idealized van der Waals expression. If the initial gap distance is 100 nm, which is in the transition range between the Casimir and van der Waals forces, the detachment length calculated from the Lifshitz formula deviates more than 30% from the values obtained from the idealized expressions.

4.3. Effects of thin SiO_2 layer on M/NEM devices

In experiments, a dielectric layer such as SiO_2 is typically used in M/NEM devices made of gold plates in order to avoid stiction of the movable part to the ground plate. The dielectric layer decreases the effect of the intermolecular forces by attenuating some of the field mode frequencies as they pass through it. Consequently, the device has a larger movable range and higher pull-in voltage.

The lines with open circles from figure 6 to figure 10 show the pull-in behaviour of two semi-infinite SiO_2 plates. The pull-in gap and pull-in voltage patterns between the line of the semi-infinite gold plates and the semi-infinite SiO_2 plates depend on the thickness of the SiO_2 layers. If the thickness of the SiO_2 layers is larger than its plasma wavelength, they act like semi-infinite SiO_2 plates. As the thickness of the SiO_2 layers decreases, the effect decreases, resulting in convergence with the line of the semi-infinite gold plates. By comparing the pull-in behaviour of the semi-infinite gold plates to those of the SiO_2 plates, shown in figures 6–10, the effect of the SiO_2 layer on the gold plates can be predicted. Even though the calculations in this paper are limited to two extreme cases (semi-infinite gold and SiO_2 plates), useful insights can be gained into the effect of a thin SiO_2 layer on gold plates.

4.4. Dynamic response of M/NEM devices

M/NEM devices exhibit nonlinear oscillations due to intrinsic nonlinearity in the intermolecular and electrostatic forces. One of the unique characteristics of nonlinear oscillations is the dc/ac symmetry-breaking phenomenon. The system is considered to have dc/ac symmetry if an orbit (the path of the device in the phase plot) is symmetric with respect to both axes in the phase plot. Thus, symmetry-breaking in dc/ac voltages is defined as the geometrical changes of an orbit with applied dc and the ac voltages. Previously, De *et al* reported that dc and ac voltages beyond the symmetry breaking points lead the system into a cascade of period doubling bifurcations [51]. A period doubling bifurcation in a dynamic system is one in which the system switches to a new behaviour with twice the period of the original system. They also showed that multiple oscillations are caused by the quadratic and cubic terms that arise from the electrostatic force. Therefore, the nonlinearity of the electrostatic force is a major source of the complex oscillations in microscale devices [47].

However, as the size of M/NEM devices decreases, the effect from the intermolecular force will be comparable to or dominant over the electrostatic force. For example, the nonlinear terms in the governing equation are expanded by using the Taylor series expansion as

$$\ddot{x} + 2\varsigma\omega_0\dot{x} + \omega_0^2 x = \frac{\varepsilon A}{2m(l-x)^2}\left(V_{dc} + V_{ac}\cos(\omega t)\right)^2 + \frac{C_n}{m(l-x)^n}. \quad (25)$$

where $F_{\text{int}}/m = C_n/\left(m(l-x)^n\right)$ is the intermolecular force. The force can either be the idealized van der Waals or Casimir

force, depending on the coefficient $n(-3$ or $-4)$.

$$\ddot{x} + 2\varsigma\omega_0\dot{x} + \omega_0^2 x = C_v\left(1+2\left(\frac{x}{l}\right) + 3\left(\frac{x}{l}\right)^2 + 4\left(\frac{x}{l}\right)^3 + \ldots\right) + \tilde{C}_n\left(1 - n\left(\frac{x}{l}\right) + \frac{n(n-1)}{2!}\left(\frac{x}{l}\right)^2\right) - \frac{n(n-1)(n-2)}{3!}\left(\frac{x}{l}\right)^3 + \ldots \quad (26)$$

where

$$C_v = \frac{\varepsilon A}{2ml^2}\left(V_{dc} + V_{ac}\cos(\omega t)\right)^2,$$
$$\tilde{C}_n = \frac{C_n}{ml^n}. \quad (27)$$

This can be arranged as:

$$\ddot{x} + 2\varsigma\omega_0\dot{x} + x\left(\omega_0^2 - \frac{2C_v}{l} - \frac{n\tilde{C}_n}{l}\right) - x^2\left(\frac{3C_v}{l^2} + \frac{n(n-1)\tilde{C}_n}{2!l^2}\right) - x^3\left(\frac{4C_v}{l^3} + \frac{n(n-1)(n-2)\tilde{C}_n}{3!l^3}\right) + \ldots = C_v + \tilde{C}_n. \quad (28)$$

When the order of magnitude of the intermolecular and electrostatic forces is similar, the ratio between the quadratic and cubic terms of equation (28) will change, altering significantly the nature of the dynamic behaviour of the system. In addition, the intermolecular force from the Lifshitz formula, which changes its slope smoothly from −3 to −4, makes it harder to analytically predict the dynamic response compared to the results from the idealized van der Waals and Casimir force expressions.

The time responses of the MSD model under the harmonic electrostatic force and the Lifshitz formula are numerically analyzed using Fast Fourier Transform (FFT) in order to explain the generation of the complex oscillations and the effect from the intermolecular force. Figure 11 shows the variation in normalized amplitude of the 1st, 2nd and 3rd modes for the fixed-fixed beam with respect to the normalized excitation frequency for two different gap distances: (a) 200 nm and (b) 50 nm. The normalized amplitude is the amplitude over the gap distance, and the normalized excitation frequency is defined as the ratio of the applied frequency ω over the resonant frequency of the switch ω_0. The applied dc and ac voltages are $V_{dc} = 0.26$ V and $V_{ac} = 0.26$ V respectively, and the other parameters used in the MSD model are taken from [47].

When the gap distance is 200 nm, the amplitude of the 2nd mode is comparable to that of the 1st, when the normalized excitation frequency is 0.5. In this case, we can see subharmonic multiple oscillations in the time response, as

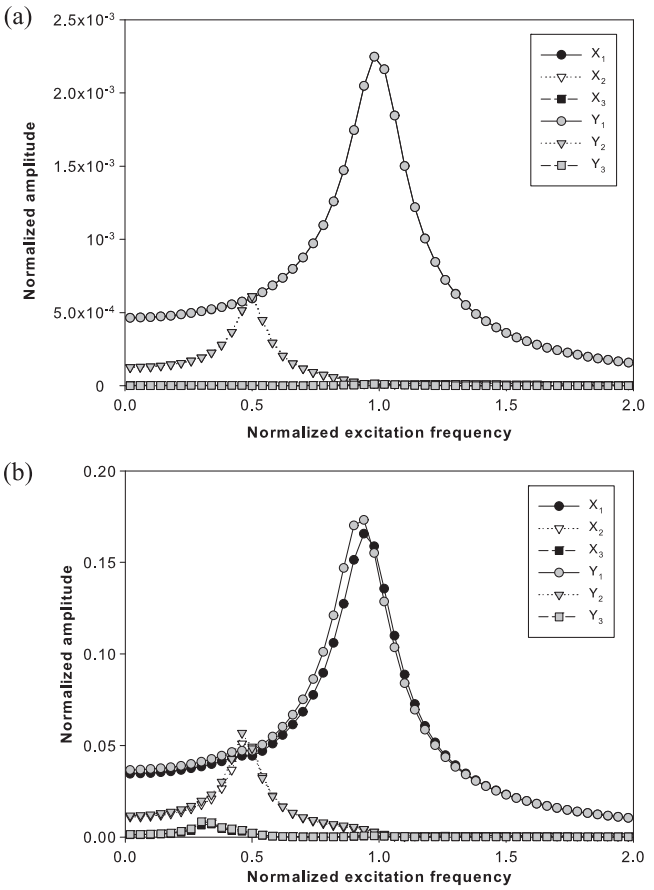

Figure 11. The variation in normalized amplitude of the 1st, 2nd and 3rd modes for the fixed-fixed beam with respect to the excitation frequency for two different gap distances ((a) 200 nm, and (b) 50 nm). X and Y are the amplitudes without and with the intermolecular force, respectively. The subscripts represent the mode numbers.

described in [51]. The Casimir force is not a dominant force in this case because the gap distance is large. Therefore, the normalized amplitudes of the 1st, 2nd and 3rd modes with and without the intermolecular force are equal, as shown in figure 11(a). When the gap is 50 nm, the 2nd mode amplitude is higher than the 1st mode, and the amplitude of the 3rd mode is also comparable to those of the 1st and 2nd when the frequency is small. Thus, we can see multiple oscillations in one period due to the similarity of the magnitude of the modes. Also, the intermolecular force becomes comparable to and even dominant over the electrostatic force at small gap distances. As we can clearly see in figure 11(b), the intermolecular force not only changes the oscillation patterns, but also lowers the resonant frequency of the device. Therefore, in dynamic response it is important to calculate the intermolecular force with the Lifshitz formula when the initial gap distance is in the transition region.

5. Conclusions

In this work, the effect of the intermolecular force on the static/dynamic pull-in behaviour is studied in the transition

region (between 10 nm to 1 μm). The intermolecular force is numerically obtained by using the Lifshitz formula and compared with the results from the idealized expressions of the van der Waals and Casimir forces. The dielectric permittivities of metals and dielectrics are numerically calculated using the dispersion relation in order to get the force from the Lifshitz formula. A significant (more than 20%) deviation in the pull-in parameters (pull-in voltage, pull-in gap, and detachment length) is observed between the results from the Lifshitz formula and idealized expressions, indicating that a more careful calculation of the intermolecular force needs to be carried out in the transition region. The effect of the deposited dielectric layers (SiO_2) on M/NEM devices (Au) is explained by showing the reduction of the intermolecular force between the two metal plates coated with a thin dielectric layer. In addition to the static cases, the dynamic response of M/NEM devices is studied. Addition of the intermolecular force changes the nature of nonlinear oscillations. We believe that the analysis performed in this work is a valuable tool for predicting the pull-in behaviour and dynamic response of M/NEM devices operating in the transition region.

Acknowledgments

The research was suppported by the National Science Foundation under grant numbers 1127480 and 1402915.

References

[1] Casimir H B G 1948 On the attraction between two perfectly conducting plates *Proc. K. Ned. Akad. Wet.* **51** 793
[2] Lifshitz E 1956 The theory of molecular attractive forces between solids *Sov. Phys. JETP* **2** 73
[3] Landau L D, Lifshitz E M and Pitaevskii L P 1984 *Electrodynamics of Continuous Media* (New York: Pergamon Press)
[4] Jackson J D 1975 *Classical Electrodynamics* (New York: Wiley)
[5] Senturia S D 2001 *Microsystem Design* (Boston: Kluwer Academic)
[6] Serry F M, Walliser D and Maclay G J 1998 The role of the Casimir effect in the static deflection and stiction of membrane strips in microelectromechanical systems (MEMS) *J. Appl. Phys.* **84** 2501–6
[7] Ding J-N, Wen S-Z and Meng Y-G 2001 Theoretical study of the sticking of a membrane strip in MEMS under the Casimir effect *J. Micromech. Microeng.* **11** 202
[8] Wang C, Guo W and Feng Q 2005 Deflection and stability of membrane structures under electrostatic and Casimir forces in microelectromechanical systems *Acta Mech.* **180** 49–60
[9] Buks E and Roukes M 2001 Stiction, adhesion energy, and the Casimir effect in micromechanical systems *Phys. Rev.* B **63** 033402
[10] van Spengen W M, Puers R and De Wolf I 2002 A physical model to predict stiction in MEMS *J. Micromech. Microeng.* **12** 702
[11] Dequesnes M, Rotkin S and Aluru N 2002 Calculation of pull-in voltages for carbon-nanotube-based nanoelectromechanical switches *Nanotechnology* **13** 120
[12] Dequesnes M, Tang Z and Aluru N 2004 Static and Dynamic Analysis of Carbon Nanotube-Based Switches *Journal of Engineering Materials and Technology* **126** 230
[13] Guo J-G and Zhao Y-P 2004 Influence of van der Waals and Casimir forces on electrostatic torsional actuators *J. Microelectromech. Syst.* **13** 1027–35
[14] Palasantzas G and De Hosson J T M 2005 Pull-in characteristics of electromechanical switches in the presence of Casimir forces: Influence of self-affine surface roughness *Phys. Rev.* B **72** 115426
[15] Lin W-H and Zhao Y-P 2005 Nonlinear behavior for nanoscale electrostatic actuators with Casimir force *Chaos, Solitons & Fractals* **23** 1777–85
[16] Ramezani A and Alasty A 2009 Instability of nanocantilever arrays in electrostatic and van der Waals interactions *J. Phys. D: Appl. Phys.* **42** 225506
[17] Ramezani A, Alasty A and Akbari J 2007 Closed-form solutions of the pull-in instability in nano-cantilevers under electrostatic and intermolecular surface forces *Int. J. Solids Struct.* **44** 4925–41
[18] Ramezani A, Alasty A and Akbari J 2008 Closed-form approximation and numerical validation of the influence of van der Waals force on electrostatic cantilevers at nano-scale separations *Nanotechnology* **19** 015501
[19] Ramezani A and Alasty A 2010 Combined action of Casimir and electrostatic forces on nanocantilever arrays *Acta Mech.* **212** 305–17
[20] Batra R, Porfiri M and Spinello D 2007 Effects of Casimir force on pull-in instability in micromembranes *EPL (Europhysics Letters)* **77** 20010
[21] Batra R, Porfiri M and Spinello D 2008 Reduced-order models for microelectromechanical rectangular and circular plates incorporating the Casimir force *Int. J. Solids Struct.* **45** 3558–83
[22] Batra R, Porfiri M and Spinello D 2008 Vibrations and pull-in instabilities of microelectromechanical von Kármán elliptic plates incorporating the Casimir force *J. Sound Vib.* **315** 939–60
[23] Zand M M and Ahmadian M 2010 Dynamic pull-in instability of electrostatically actuated beams incorporating Casimir and van der Waals forces *J. Mech. Eng. Sci.* **224** pp 2037–47
[24] Wang Y-G, Lin W-H, Li X-M and Feng Z-J 2011 Bending and vibration of an electrostatically actuated circular microplate in presence of Casimir force *Appl. Math. Modelling* **35** 2348–57
[25] Koochi A, Fazli N and Rach R 2014 Modeling the pull-in instability of the CNT-based probe/actuator under the Coulomb force and the van der Waals attraction *Latin American J. Solids Struct.* **11** 1315–28
[26] Rodriguez A W, Capasso F and Johnson S G 2011 The Casimir effect in microstructured geometries *Nat. Photonics* **5** 211–21
[27] Berman D and Krim J 2013 Surface science, MEMS and NEMS: progress and opportunities for surface science research performed on, or by, microdevices *Prog. Surf. Sci.* **88** 171–211
[28] Zhang W-M, Yan H, Peng Z-K and Meng G 2014 Electrostatic pull-in instability in MEMS/NEMS: A review *Sens. Actuators A: Physical* **214** 187–218
[29] Zhou F and Spruch L 1995 van der Waals and retardation (Casimir) interactions of an electron or an atom with multilayered walls *Phys. Rev.* A **52** 297
[30] Jaffe R 2005 Casimir effect and the quantum vacuum *Phys. Rev.* D **72** 021301
[31] Bordag M, Mohideen U and Mostepanenko V M 2001 New developments in the Casimir effect *Phys. Rep.* **353** 1–205
[32] Milonni P W 1994 *The Quantum Vacuum: an Introduction to Quantum Electrodynamics* (San Diego, CA: Academic)

[33] Lamoreaux S K 2005 The Casimir force: background, experiments, and applications *Rep. Prog. Phys.* **68** 201
[34] Van Kampen N, Nijboer B and Schram K 1968 On the macroscopic theory of van der Waals forces *Phys. Lett.* A **26** 307–8
[35] Lambrecht A and Reynaud S 2000 Casimir force between metallic mirrors *Euro. Phys. J.* D **8** 309–18
[36] Brevik I, Aarseth J, Høye J and Milton K 2005 Temperature dependence of the Casimir effect *Phys. Rev.* E **71** 056101
[37] Bezerra V, Klimchitskaya G, Mostepanenko V and Romero C 2004 Violation of the Nernst heat theorem in the theory of the thermal Casimir force between Drude metals *Phys. Rev.* A **69** 022119
[38] Decca R, López D, Fischbach E, Klimchitskaya G, Krause D and Mostepanenko V 2007 Novel constraints on light elementary particles and extra-dimensional physics from the Casimir effect *Euro. Phys. J.* C **51** 963–75
[39] Geyer B, Klimchitskaya G and Mostepanenko V 2007 Generalized plasma-like permittivity and thermal Casimir force between real metals *J. Phys. A: Math. Theor.* **40** 13485
[40] Svetovoy V, Van Zwol P, Palasantzas G and De Hosson J T M 2008 Optical properties of gold films and the Casimir force *Phys. Rev.* B **77** 035439
[41] Broer W, Palasantzas G, Knoester J and Svetovoy V B 2013 Significance of the Casimir force and surface roughness for actuation dynamics of MEMS *Phys. Rev.* B **87** 125413
[42] Klimchitskaya G, Mohideen U and Mostepanenko V 2009 The Casimir force between real materials: experiment and theory *Rev. Mod. Phys.* **81** 1827
[43] Palik E D 1998 *Handbook of Optical Constants of Solids* (New York: Academic)
[44] Bergström L 1997 Hamaker constants of inorganic materials *Adv. Colloid Interface Sci.* **70** 125–69
[45] Parsegian V A and Ninham B 1970 Temperature-dependent van der Waals forces *Biophys. J.* **10** 664–74
[46] Nathanson H C, Newell W E, Wickstrom R A and Davis J R Jr 1967 The resonant gate transistor *Electron Devices, IEEE Transactions on* **14** 117–33
[47] De S K and Aluru N 2006 Complex nonlinear oscillations in electrostatically actuated microstructures *J. Microelectromech. Syst.* **15** 355–69
[48] Zhu Y, Ke C and Espinosa H 2007 Experimental techniques for the mechanical characterization of one-dimensional nanostructures *Exp. Mech.* **47** 7–24
[49] Ke C, Espinosa H and Pugno N 2004 A feedback controlled carbon nanotube based NEMS device *Proc. Int. Conf. Exp. Mech. 12* (*Bari Italy, August 29–September 2*)
[50] Lin W-H and Zhao Y-P 2005 Casimir effect on the pull-in parameters of nanometer switches *Microsyst. Technol.* **11** 80–5
[51] De S K and Aluru N 2005 Complex oscillations and chaos in electrostatic microelectromechanical systems under superharmonic excitations *Phys. Rev. Lett.* **94** 204101